HHS Public Access

Author manuscript

Cancer Res. Author manuscript; available in PMC 2018 March 15.

Published in final edited form as:

Cancer Res. 2017 March 15; 77(6): 1345–1356. doi:10.1158/0008-5472.CAN-16-0785.

RelB expression determines the differential effects of ascorbic acid in normal and cancer cells

Xiaowei Wei[1,4], **Yong Xu**[1,4], **Fang Fang Xu**[2], **Luksana Chaiswing**[1], **David Schnell**[1], **Teresa Noel**[1], **Chi Wang**[3], **Jinfei Chen**[4,*], **Daret K. St Clair**[1,*], and **William H. St Clair**[2,*]

[1]Department of Toxicology and Cancer Biology, University of Kentucky, Lexington, Kentucky 40536, USA

[2]Department of Radiation Medicine, University of Kentucky, Lexington, Kentucky 40536, USA

[3]Biostatistics Core, Markey Cancer Center, University of Kentucky, Lexington, Kentucky 40536, USA

[4]Department of Oncology, Nanjing First Hospital, Nanjing Medical University, Nanjing, China, 210006

Abstract

Cancer cells typically experience higher oxidative stress than normal cells, such that elevating pro-oxidant levels can trigger cancer cell death. Although pre-exposure to mild oxidative agents will sensitize cancer cells to radiation, this pre-exposure may also activate the adaptive stress defense system in normal cells. Ascorbic acid (AA) is a prototype redox modulator that when infused intravenously appears to kill cancers without injury to normal tissues; however, the mechanisms involved remain elusive. In this study, we show how AA kills cancer cells and sensitizes prostate cancer to radiation therapy, while also conferring protection upon normal prostate epithelial cells against radiation-induced injury. We found that the NF-κB transcription factor RelB is a pivotal determinant in the differential radiosensitization effects of AA in prostate cancer cells and normal prostate epithelial cells. Mechanistically, high ROS concentrations suppress RelB in cancer cells. RelB suppression decreases expression of the sirtuin SIRT3 and the powerful antioxidant MnSOD, which in turn increases oxidative and metabolic stresses in prostate cancer cells. In contrast, AA enhances RelB expression in normal cells, improving antioxidant and metabolic defenses against radiation injury. In addition to showing how RelB mediates the differential effects of AA on cancer and normal tissue radiosensitivities, our work also provides a proof of concept for the existence of redox modulators that can improve the efficacy of radiotherapy while protecting against normal tissue injury in cancer settings.

Corresponding Authors: Daret K. St. Clair, PhD, Department of Toxicology and Cancer Biology, University of Kentucky, 1095 VA Drive, Lexington, KY 40536, Phone 859-257-3956, Fax 859-323-1059, dstcl00@uky.edu; William H. St. Clair, MD, PhD, Department of Radiation Medicine, University of Kentucky, 800 Rose Street, Lexington, Kentucky 40536, Phone 859-323-6486, Fax 859-257-4931, stclair@uky.edu; Jinfei Chen, MD, Department of Oncology, Nanjing First Hospital, Nanjing Medical University, 68 Changle Road, Nanjing, Jiangsu Province, P.R. China. phone:+86-025-87726234, fax:+86-025-87726234, jinfeichen@sohu.com.

Disclosure of Potential Conflicts of Interest

The authors have no potential conflicts of interest to disclose.

Keywords

RelB; ascorbic acid; prostate cancer; radiotherapy

Introduction

Prostate cancer is the most prevalent cancer in the United States and is the second leading cause of cancer deaths in men (1). The predominant prostate cancer therapy, ionizing radiation (IR), is used to treat more than 750,000 patients per year (2). Unfortunately, the therapeutic efficacy of IR tends to decrease when cancer cells develop adaptive responses to resist it. Even with modern conformal radiation therapy, biochemical failure occurs in approximately 45% of patients with a locally confined disease (3). Additionally, corresponding with the widespread use of high-dose IR to treat prostate cancer, the incidence of radiation-related genitourinary toxicity has increased (4). Therefore, novel therapeutic strategies to enhance both radiosensitization in cancer cells and radioprotection in normal tissues are urgently needed.

Cancer cells are usually under higher oxidative stress than normal cells, and cellular redox state is thought to be important to cell fate. The level of oxidative stress is also critical to radiation response (5, 6). In addition to directly damaging DNA, IR can produce a large amount of free radicals that cause cell death (5). Due to water radiolysis, IR causes excess superoxide generation and allows leakage of electrons from the electron transport chain (ETC), resulting in mitochondrial dysfunction (7). However, IR also tends to induce adaptive reactive oxygen species (ROS) defense systems in cancers, which may lead to radioresistance (8). While increasing radiation intensity can improve the ability to control cancer growth, it presents the significant risks of increasing unwanted side effects, including injury to normal tissues and reduced quality of life for cancer survivors. Thus, an attractive radiation therapy would be one that exploits the intrinsic differences in the cellular redox statuses of normal cells and cancer cells by selectively boosting ROS generation in cancer cells to push them into oxidative stress overload while stimulating adaptive responses in normal cells.

Ascorbic acid (AA), better known as vitamin C, has a somewhat controversial history as a therapeutic drug for cancer treatment (9, 10). Emerging studies suggest that only intraperitoneal or intravenous AA, and not orally administered AA, can reach pharmacological concentrations that kill cancer (10, 11). However, although clinical trials of AA have demonstrated the differences between administration routes and the safety of intravenous AA (12, 13), there is still a lack in understanding the mechanisms by which AA kills cancer cells. In general, the cytotoxicity induced by AA seems to be primarily mediated by hydrogen peroxide (H_2O_2) generated in extracellular fluids (14). A recent elegant study demonstrated that pharmacologic ascorbate enhances the cytotoxic effects of ionizing radiation in pancreatic cancer cell lines, but not in nontumorigenic pancreatic ductal epithelial cells because pancreatic cancer is sensitive to H_2O_2 (15). Thus, the cytotoxic effect of AA may well be dependent on the local redox environment of the cancer cells.

Mounting evidence suggests that ROS-mediated NF-κB activation is involved in the radiation resistance of cancers (16). The NF-κB family includes NF-κB1 (p50/p105), NF-κB2 (p52/p100), c-Rel, RelA (p65), and RelB. Recent studies have demonstrated that RelB is uniquely expressed at a high level in prostate cancer with high Gleason scores, suggesting that RelB plays an important role in the radioresistance of prostate cancer (17, 18). The present study examined the effects of AA on cell survival and on the responses to radiation of prostate cancer cells and normal prostate epithelial cells *in vitro* and *in vivo*. We found that the intrinsic differences in the cellular redox state of normal and cancer cells account, in part, for the differential effects of AA on the modulation of cellular redox status. The expression of RelB in normal and cancer cells serves as a central regulator for their opposing responses to radiotherapy.

Materials and Methods

Cell culture, cell transfection, and reagents

Human prostate cancer cell lines LNCaP and PC3, as well as normal human prostate epithelial viral transformed PZ-HPV-7 (PZ) cells, were obtained from American Type Culture Collection. These cell lines are routinely checked for morphological and growth changes to probe for cross-contaminated or genetically drifted cells. All cell lines used have been reauthenticated using the Short Tandem Repeat (STR) profiling service by ATCC. Normal human epithelial cells (PrEC) were purchased from Lonza. The cells were cultured and maintained in the manufacturer's suggested media. Plasmid-cloned RelB cDNA and siRNA for knocking down RelB were transfected into LNCaP and PC3 cells using a Lipofectamine 2000 kit (Life Technologies) according to the manufacturer's instructions. AA (powder, USP/FCC grade, Fisher Chemical) was prepared as a 1 M stock solution in sterile water, with sodium hydroxide added dropwise to adjust the pH to 7.0, as previously described. H_2O_2 (Sigma) solutions were prepared freshly prior to application to the cells.

Treatment and cell survival analysis

Cell survival rates were quantified by colony survival and MTT assays. For colony survival analyses, the cells were plated in 6-well plates at low densities and then treated with 0 to 1.0 mM AA for 2 h, which corresponds to the clinical time course of intravenous AA administration (19). The formed colonies were washed with 1×PBS and stained with a crystal violet dye for clonogenic assay. The surviving fraction was calculated as the ratio of the number of colonies formed to the number of cells effectively plated.

For the MTT assay, cells were seeded in flat-bottomed 96-well plates, treated with 0 to 64 mM AA for 2 h, washed with fresh media, and incubated for 2 doubling times in the absence of AA. Cell viability was detected by an MTT assay kit (Trevigen) following the standard protocol. The IC_{50} for each cell line was calculated from a dose-response curve using GraphPad Prism 6.0 software (GraphPad software). For evaluations of combination therapy, PC3 and PZ cells were treated with AA, IR or a combination of the two. IR was performed at 1 h after AA treatment by a 250 kV X-ray machine (Faxitron X-ray Corp.) with peak energy of 120 kV, 0.05 mm Al filter, at a dose of 0 to 6 Gy. After total 2 h exposure to AA, cells were incubated for 2 doubling times in the absence of AA and assessed by MTT assay.

Combination Index (CI) values were calculated by CompuSyn 1.0 (CompuSyn) and the effects of combined IR and AA treatment were evaluated according to the acknowledged range of CI as published (20).

Animals

Four- to five-week-old male NCRNU (nu/nu athymic nude) mice were obtained from Taconic (Hudson). For formation of xenograft tumors, 1.8×10^6 cells mixed in Matrigel (BD Biosciences) were subcutaneously injected into the right flanks of the mice. Tumor volumes were routinely measured and their sizes calculated on the basis of a protocol described elsewhere (21). Animals with an average tumor size of 350 mm^3 were randomized into 4 groups (n=10) and treatment commenced with intraperitoneal injection as follows: (i) control, saline once daily; (ii) AA, 4.5 g/kg once daily; (iii) IR, 2 Gy once every other day; (iv) IR+AA. The dosage of AA was determined by conversion of clinical trial data and with reference to recent studies (22). For combination treatments, IR was performed at 1 h after AA injection. After treatment, the mice were observed daily and humanely killed when the tumor reached the maximum size of 1500 mm^3. The tumor, prostate, and bladder tissues were collected for protein and RNA analysis. All animal experimental procedures were approved by the Institutional Animal Care and Use Committee of the University of Kentucky (Lexington, KY), Approval Protocol No. 01077M2006.

Quantification of ROS level

An Amplex Red assay was used to quantify the levels of extracellular H_2O_2 after AA and IR treatments. Briefly, cells were incubated with 50 μM Amplex Red reagent (ThermoFisher) at 37°C for 10 min. Fluorescence was detected at ex/em 550/590 nm using a Gemini XPS Microplate Reader (Molecular Devices). The extracellular H_2O_2 level was calculated by a standard curve and normalized to the cell number. MitoSox Red (ThermoFisher), a highly selective mitochondrial superoxide indicator for live cells, was used to estimate the levels of superoxide, and Mitotracker green FM (ThermoFisher) was used to locate mitochondria. Rotenone (200 nM, Sigma), known to be a mitochondrial superoxide inducer, was used as a positive control. To account for superoxide-specific fluorescence, the cells were pretreated with 100 units/mL PEG-SOD (Sigma) for 24 h followed by the treatment. In brief, cells were loaded with Mitotracker Green at 100 nM for 15 min followed by 5 μM MitoSox Red for 10 min at 37°C and rinsed 3 times with HBSS before measuring fluorescence. Cellular fluorescence intensity was detected using an Olympus IX71 fluorescence microscope and a Gemini XPS Microplate Reader at ex/em 510/580 nm.

Catalase and MnSOD treatments

To further determine the specific high ROS level induced by AA and radiation, PC3 cells were treated with various forms of catalase or MnSOD, including catalase (100u/mL), PEG-CAT (200 U/mL), PEG-MnSOD (100 U/mL) or adenovirus MnSOD. Catalase, PEG-catalase and PEG-MnSOD were purchased from Sigma-Aldrich. For the adenovirus experiments, viral vectors utilized included AdCMVEmpty (AdEmpty) and AdCMVMnSOD (AdMnSOD), manufactured by Viraquest, Inc. (North Liberty, IA) as previously described (23, 24). Approximately 10^6 PC3 cells were plated in a 100 mm2 tissue culture dish and incubated with the adenovirus constructs for 24 h. Media were replaced

with 5 mL of complete media for an additional 24 h before cells were harvested for MTT assay or treated for ROS measurements.

Measurement of oxygen consumption rates, ATP, and lactate production

To determine whether AA changes mitochondrial function in cancer and normal cells, a Seahorse Bioscience XF96 Extracellular Flux Analyzer was used to measure oxygen consumption rates (OCR) after 2 h of treatment with 4 mM AA. The data were normalized with protein levels and expressed as the OCR in pmol/min/μg protein. Cellular ATP concentrations were measured using an ATP Assay kit (Biomedical Research Service Center). Extracellular and intracellular lactate levels were measured by a Lactate Assay kit (Biomedical Research Service Center). Data were normalized to the cell number, as indicated in each figure.

Western blots

Lysates from homogenized cells and tumor tissues were electrophoresed on a 10–12% (w/v) SDS-PAGE gel, transferred onto a nitrocellulose membrane, and subsequently incubated with primary antibodies against RelA, RelB, Bcl-xl, Bax, or GAPDH from Santa Cruz Biotech, or SIRT1 (Upstate Biotech), MnSOD (Upstate Biotech), SIRT3 (Cell Signaling), or β-actin (Sigma). All secondary antibodies were obtained from Santa Cruz Biotech. The blots were visualized using an enhanced chemiluminescence detection system (Amersham Pharmacia Biotech).

Real-time PCR

mRNA was isolated from cells and tissues using a MagNA Pure Compact RNA Isolation Kit (Roche) and reverse-transcribed using a Taqman reverse transcription kit (ThermoFisher) according to the manufacturer's instructions, and then analyzed using a LightCycler® 480 Real-Time PCR System (RT-PCR, Roche) with gene-specific primers. All primers were purchased from Invitrogen. Primer sequences for human genes were as follows:

RELB 5′-cacttcctgcccaaccac-3′ (forward) and 5′-gacacggtgccagagaaga-3′ (reverse); Bcl-xl 5′-agccttggatccaggagaa-3′ (forward) and 5′-gctgcattgttcccatagagt-3′ (reverse); *SIRT3* 5′-cttgctgcatgtggttgatt-3′ (forward) and 5′-cggtcaagctggcaaaag-3′ (reverse); β-actin 5′-ccaaccgcgagaagatga-3′ (forward) and 5′-ccagaggcgtacagggatag-3′ (reverse).

Primer sequences for mouse genes were as follows:

RelB 5′-gtgacctctcttccctgtcact-3′ (forward) and 5′-tgtattcgtcgatgatttccaa-3′ (reverse); *Sirt3* 5′-tcctctgaaaccggatgg-3′ (forward) and 5′-tcccacacagagggatatgg-3′ (reverse); β-actin 5′-ctggctcctagcaccatga-3′ (forward) and 5′-acagtgaggccaagatggag-3′ (reverse).

NF-κB binding assay

Nuclear extracts from the treated and untreated PC3 and PZ cells were prepared by a nuclear extract kit (Active Motif). Binding activities of RelA and RelB were measured using an

ELISA-based TransAM NF-κB Family kit (Active Motif) according to the manufacturer's protocol.

Chromatin immunoprecipitation

A Pierce™ Agarose ChIP Kit (ThermoFisher) was used to study RelB-mediated transcriptional regulation according to the manufacturer's protocol. A potential RelB binding site was predicted in the promoter region of the human *SIRT3* gene based on a search of the Ensembl genome database and a recent study (25). Briefly, chromatin was pulled down using a RelB antibody (Santa Cruz Biotech), and a DNA fragment containing an NF-κB element located in the *SIRT3* promoter region was analyzed by quantitative PCR (qPCR) with LightCycler® 480 SYBR Green I Master kit (Roche). PCR primer sequences for *SIRT3* were 5′-gaattatgaaatgagcacag-3′ (forward) and 5′-caggatagcaagaacgagca-3′ (reverse). Rabbit IgG antibody was used as a negative control. ChIP-qPCR data were normalized by input preparation.

Intracellular Catalase, Gpx and MnSOD enzymatic assay

The activities of catalase and Gpx were measured by a Catalase- specific activity assay kit (Abcam) and a Gpx Cellular activity assay Kit (Sigma) according to the manufacturers' protocols, respectively. MnSOD activities were measured by the nitroblue tetrazolium-bathocuproin sulfonate reduction inhibition method. Sodium cyanide (2 mM) was used to inhibit CuZnSOD activity as a previous study described (26).

Quantitative and statistical data analyses

Multiple independent experiments were conducted for each set of data presented. Image data were quantified using the quantitative imaging software Image-pro Plus 6.0 (Media Cybernetics). Toxicity comparisons of multiple groups were analyzed using ANOVA and a post-hoc test. Data represent the mean ± SEM. Kaplan-Meier survival curves and the log-rank test were performed for comparison of the survival curves in animal experiments. Statistical significances of other experiments were analyzed using one-way ANOVA and Tukey's multiple comparison tests. All analyses were performed with IBM SPSS 21.0 software (Microsoft). Differences with an associated $P < 0.05$ were considered to be significant.

Results

AA enhances radiosensitivity in prostate cancer cells but protects normal cells from radiotoxicity

To determine the cytotoxicity of AA in prostate cancer and normal cells, LNCaP, PC3, PrEC, and PZ cells were plated for colony survival assays and MTT assays. As shown in Fig. 1A and B, high doses of AA alone efficiently killed cancer cells but exerted no or minimal effect on normal cells. Interestingly, AA appears to be more efficient in killing aggressive prostate cancer PC3 cells than LNCaP cells. Based on a dose-effect curve, the IC_{50} values for PC3, LNCaP, PrEC, and PZ cell lines were quantified as 3.96 mM, 12.81 mM, 36.56 mM, and 33.79 mM, respectively, indicating that AA has different cytotoxic effects on prostate cancer and normal cells.

To determine the capacity of AA to sensitize prostate cancer cells to IR, we used the protocol for radiosensitization of PC3 cells described in our previous study (27), taking into consideration the relative AA IC_{50} value in clinical application (28). The total dose of AA was kept at 2 mM (for 1/2 IC_{50}) or 4 mM (for the full IC_{50}). Pretreatment with AA significantly increased the radiosensitivity of PC3 cells in a dose-dependent manner within an IR range of 0.5 to 6 Gy (Fig. 1C). Interestingly, pretreatment with AA resulted in the opposite effect in PZ cells, indicating that AA actually protects normal cells against the cytotoxicity induced by IR (Fig. 1C). To assess the combined effects of AA and IR, the CI value for each dose was calculated by CompuSyn software based on the Chou-Talalay method (20). A dose of 4 mM AA conformed to the Cl range description, in that it displayed a synergistic effect on IR from 1 to 6 Gy in PC3 cells (Table S1). On the contrary, both doses of AA in PZ cells displayed antagonistic effects on IR over a dose range of 0.5 to 6 Gy. These results suggest that equivalent pharmacological doses of AA can exert different radiosensitization effects in prostate cancer and normal cells.

AA differentially modulates cellular ROS levels in cancer and normal cells

To determine the effect of AA on redox homeostasis in cancer and normal cells, the levels of ROS and mitochondrial superoxide anion were measured with and without AA treatment. As shown in Fig. 2A, the basal level of extracellular H_2O_2 was slightly but significantly higher in prostate cancer cells than in normal cells. In comparison to the result in PZ cells, AA treatment induced a significant increase in ROS in prostate cancer cells, especially PC3 cells (Fig 2A). Pretreatment with PEG-Catalase or catalase obviously inhibited such extracellular H_2O_2 increases and weakened toxicity of AA in PC3 cells (Fig. S1A and B). These results are consistent with previous reports that AA produces H_2O_2 by oxidative reaction with metal ions in extracellular fluid and exerts cytotoxic effects (14, 15).

To evaluate intracellular redox status, superoxide levels in mitochondria, the primary source of cellular ROS, were quantified in cancer and normal cells. Mitotracker green staining with negligible stimulated ROS was used to normalize MitoSox red to quantify mitochondrial superoxide anion induced by AA with rotenone as a positive control. AA induced superoxide generation in PC3 cells, but the effect was mitigated by adding PEG-SOD (Fig. S1C). Consistent with the results for cytotoxicity in Fig. 1, AA increased IR-induced superoxide generation in PC3 cells but decreased it in PZ cells (Fig. 2B). Increasing endogenous MnSOD expression in PC3 cells clearly decreased superoxide, especially IR-induced superoxide generation after AA treatment (Fig S1D). These results suggest that AA amplifies IR-induced cellular ROS level in cancer cells. They also suggest that AA suppresses IR-induced ROS generation in normal cells.

AA differentially modulates mitochondrial function in cancer and normal cells

To test whether altering cellular redox status is associated with mitochondrial function, the oxygen consumption rate (OCR) in the AA-treated cells was measured using a Seahorse Bioscience XF96 OxygenFlux Analyzer. As shown in Fig. 3A, AA treatment decreased basal, ATP-linked, and maximal OCR but not reserve capacity in PC3 cells. In contrast, AA treatment increased the maximal OCR and reserve capacity of PZ cells. To test if such effects modulate the energy production of cells, the cellular ATP and lactate levels were

determined with and without treatment. As expected, pretreatment with AA significantly diminished intracellular ATP when combined with IR, but increased both extracellular and intracellular lactate production in PC3 cells (Fig. 3B, C, D). In contrast, combined AA and IR treatment increased ATP production but decreased lactate concentrations in normal PZ cells (Fig. 3B, C, D). These results suggest that AA-mediated alterations in cellular oxidative and metabolic stresses play pivotal roles in the radiation response of both prostate cancer and normal cells. Importantly, AA exacerbates mitochondrial dysfunction in cancer cells, but alleviates radiation-induced mitochondrial dysfunction in normal cells.

AA inversely regulates RelB expression in cancer and normal cells

NF-κB signaling is involved in multiple biological processes responsive to ROS (29). The best known activator of NF-κB is RelA, which is associated with radioresistance in many types of cancer. Our previous findings demonstrate that RelB is also highly expressed in prostate cancer cells and is a major contributor to radioresistance (18, 30). To probe which member of the NF-κB family is affected by AA, we first determined whether AA regulates the expression of RelA and RelB in prostate cancer and normal cells at the mRNA and protein levels. While AA slightly increased RelA protein levels in both cancer and normal cells, AA strongly down-regulated RelB protein and mRNA in cancer cells and up-regulated RelB in normal cells (Fig. 4A). To further verify this finding, an NF-κB binding assay was performed to confirm AA activation or suppression of RelA and RelB. As shown in Fig. 4B, RelB binding activity was strongly suppressed in PC3 cells but apparently activated in PZ cells after AA treatment alone. Importantly, pretreatment with AA significantly diminished IR-induced RelB activation in PC3 cells. No significant effect of AA was observed on RelA binding activity, but a small but significant increase was observed with combination treatment in PZ cells.

To further confirm the transcription effect of RelB on its target genes, the NF-κB-regulated genes Bcl-xL and Bax were quantified to verify the regulation of the NF-κB pathway by AA in prostate cancer and normal cells. Consistently, AA down-regulated Bcl-xL but up-regulated Bax in PC3 cells, while the reverse effect of AA was observed in PZ cells (Fig. S2A). Finally, to confirm the role of RelB in AA-induced cell killing of prostate cancer cells, the level of RelB was manipulated by either overexpression of RelB in LNCaP cells or knockdown of RelB in PC3 cells. AA-mediated cytotoxicity was increased in RelB-silenced PC3 cells but reduced in RelB-overexpressed LNCaP cells (Fig. 4C, Fig. S2A).

RelB acts as a central regulator in response to oxidative and metabolic stresses in cancer cells

Generally, the radiosensitization we find in cancer cells is due to the oxidative and metabolic stresses induced by AA. Since our data showed that RelB plays an important role in AA-induced cell killing of prostate cancer cells, it was necessary to verify the functions of RelB in oxidative and metabolic stresses. As shown in Fig 5A, knockdown of RelB reduced basal ATP production and increased intracellular lactate level. When treated with AA, IR or combination treatment, RelB-silenced PC3 cells displayed more aggravated metabolic stress compared to the control group (Fig 5A). The OCR data further confirmed the effect of suppressing RelB on mitochondrial function in cancer cells, especially when treated with

AA and IR (Fig 5B). To confirm the role of RelB in response to oxidative stress, the activities of ROS related enzymes were evaluated in RelB-silenced PC3 cells. As shown in Fig 5C, 5D knocking down RelB markedly weakened the ability of ROS elimination in cancer cells which was revealed by the reduction of catalase, GPX and MnSOD activities. These results confirm the role of RelB in oxidative and metabolic regulations. Furthermore, they confirm that RelB may be a central regulator that adjudicates the differential effects of AA in normal and cancer cells.

RelB transcriptionally regulates SIRT3 in response to AA treatment

SIRT3, a member of the sirtuin family of NAD+-dependent protein deacetylases, is known to play a critical role in maintaining mitochondrial function, ROS response, and cell proliferation, as well as in inducing radioresistance in cancers. Recently, a sequential action of SIRT1-RelB-SIRT3 has been reported in sepsis (31), but the related mechanisms remain to be fully elucidated. To probe the relationship of SIRT3 with RelB in AA-induced cytotoxicity in cancer cells and the protective effect in normal cells, the levels of SIRT1 and SIRT3 relative to RelB were quantified in PC3 and PZ cells. As shown in Fig. 6A, up-regulation and down-regulation of SIRT3 correlated with RelB in the AA-treated cells, but no significant changes were observed in SIRT1. Interestingly, MnSOD, a typical NF-κB-regulated mitochondrial antioxidant enzyme, was suppressed in PC3 cells but enhanced in PZ cells treated with AA (Fig. 6A).

Manipulation of RelB expression in cancer cells altered SIRT3 levels, indicating that SIRT3 is regulated by RelB (Fig. 6B). Subsequently, RT-PCR showed that RelB transcriptionally regulated SIRT3 in the AA-treated cells (Fig. 6C). Furthermore, chromatin was pulled down by a RelB antibody, and a promoter region of the human SIRT3 gene containing a NF-κB element was quantified by qPCR (Fig. 6D). The amount of the pulled down promoter fragment was reduced by AA treatment in PC3 cells but increased in AA-treated PZ cells. When combined with IR, AA consistently suppressed the activated RelB-SIRT3 signal in cancer cells but further activated the RelB-SIRT3 signal in normal cells.

AA enhances radiosensitivity of prostate cancer *in vivo*

To further confirm our findings *in vitro*, a tumor-bearing mouse model was used to verify the effect of AA on tumor growth. Mice were subcutaneously injected with PC3 cells followed by AA and IR treatments. Mice were humanely killed and tumors as well as prostate and bladder tissues were collected when the tumor volume reached 1500 mm^3. The tumor growth rate of each group shown in Fig. 7A demonstrates the efficacy of AA in sensitizing prostate cancer to radiation therapy. There was a trend toward significance in the differences between AA-treated and untreated mice. The time needed for the tumors in each group to reach 1500 mm^3 was independently analyzed (Fig. S3A).

mRNA and protein levels of RelB and its targets, SIRT3 and MnSOD, were quantified in the extracted tumor tissues. Consistent with the results obtained *in vitro*, IR increased the levels of RelB, SIRT3, and MnSOD, but AA eliminated the increases (Fig. 7B). In addition, prostate and bladder tissues were used to probe whether AA activates a protective response

against radiation injury in normal tissues. AA increased levels of RelB and SIRT3 mRNA in normal prostate and bladder tissues (Fig. 7C).

Overall, AA enhances the radiosensitivity of prostate cancer cells but protects normal cells from radiotoxicity through RelB-dependent transcriptional regulation, with consequences for downstream target genes, such as SIRT3 and MnSOD, that lead to distinct responses to radiation, as illustrated in a working model based on the results obtained to- date (Fig. 7D).

Discussion

The problems of the radioresistance of cancer tissues and the toxic side effects of IR in normal tissues have been extensively investigated in both scientific and clinical settings. However, traditional approaches have focused on ensuring that protecting normal tissues from injury does not also reduce the therapeutic efficacy of radiation. Here, we demonstrate that AA, a redox active agent, can enhance the therapeutic efficacy of radiation therapy while simultaneously protecting normal tissues against the side effects of radiation therapy.

That AA enhances traditional radiotherapy and chemotherapy of cancer has been reported since 1977 (14,15, 32–35). In the intervening decades, AA has been used to alleviate some of the side effects of radiation therapy during cancer treatment (34, 36). A recent study by Du et al. clearly shows the radiosensitization induced by pharmacological AA in pancreatic cancer cells (15). These authors also observed that AA also potentially protects the gastrointestinal tract from IR *in vivo*. Although it was not a major focus of the study, the Du et al. observation is consistent with our finding that AA indeed protects normal prostate and bladder tissues from IR.

Elevated ROS levels, which are essential for tumorigenesis and metastasis, have been observed in many types of cancer. High levels of ROS may reveal a specific vulnerability of malignancy that can be used to selectively enhance cell death by further increasing the level of cellular ROS. Here, we show that AA acts as a prooxidant at pharmacological doses and differentially modulates cellular responses to ROS in normal and cancer cells. Our results are consistent with previous studies demonstrating that the cytotoxicity induced by AA is primarily mediated by H_2O_2 (14, 15, 19 and 22). However, the previous studies did not take into consideration the respective distinct basal redox state of normal and cancer cells. Our data suggest that AA causes an increase in ROS in prostate cancer cells that reaches a threshold level of cell death but only slightly increases ROS in normal cells, resulting in an induction of antioxidant and metabolic responses. These opposing effects of AA in normal and cancer cells are mediated in part by the expression of RelB, a member of the alternative pathway of the NF-κB family.

NF-κB is known to be an important ROS-responsive transcriptional factor involved in both tumor progression and tumor resistance to treatment (16). Previous studies have indicated that AA can inhibit NF-κB activation by preventing the degradation of IκB-α and nuclear translocation of RelA (37, 38). Recent studies by our laboratory and others have demonstrated that RelB contributes to radioresistance of prostate cancer cells by sustaining NF-κB activation (17, 18). The present study further establishes the role of RelB as a critical

redox signaling sensor that regulates its downstream target genes in response to AA, leading to the observed opposing radiation responses in prostate cancer and normal cells. Repression of IR-induced RelB activation in cancer cells results in diminished oxidative defense capacity and subsequently enhances radiosensitivity through mitochondrial dysfunction. On the contrary, up-regulation of RelB serves as a major mechanism by which AA protects normal tissues against radiotoxicity, through up-regulation of antioxidant enzymes and the mitochondrial function of scavenging ROS. RelA has been reported to be involved in RelB transcriptional activation (39); further studies will be needed to determine whether and how RelA participates in a meaningful change of RelB as it relates to AA.

Recently, metabolic alterations in cancer cells due to AA-induced oxidative stress have been the subject of intense investigation (15, 40). Although a high rate of aerobic glycolysis in tumors, known as the Warburg effect, has been observed in various types of cancer, cancers have functional mitochondria, and mitochondrial respiration is necessary for cancer cell proliferation and resistance to therapy (41, 42). The present study shows that the mitochondria in prostate cancer cells become dysfunctional, with down-regulated MnSOD, after AA treatment. As a MnSOD transcriptional regulator, RelB modulation by AA leads to the suppression and induction of MnSOD in cancer and normal cells, respectively.

Sirtuins are NAD^+-dependent histone deacetylases in mammalian cells and are involved in an array of critical cellular functions (43–46). Of the seven human sirtuins, SIRT3 is the best characterized in its regulation of many aspects of mitochondrial function. Physiologically, SIRT3 interacts with subunits of complexes I and II of the ETC to improve mitochondrial respiration (47). SIRT3 also deacetylates and activates MnSOD to maintain the antioxidant defense system in cells (48). A recent study described the expression of SIRT3 as a sequential action of the SIRT1-RelB axis in a sepsis model (31). The present study suggests that the RelB-SIRT3 signaling axis may play a critical role in AA treatment independent of SIRT1 levels. Our results demonstrate that RelB regulates SIRT3 expression through binding to its promoter region. Repression of RelB-activated SIRT3 transcription by AA aggravates metabolic stress in cancer cells. In contrast, up-regulation of SIRT3 improves the ability of mitochondria to defend against metabolic stresses in normal cells. These results suggest that RelB may be a unique target for treatment of radiation-resistant prostate cancer.

Considering the unsatisfactory results of clinical trials of high doses of oral AA, and the reported successes of high doses of intravenous ascorbate (49, 50), the complexity of the mechanisms involved in AA treatment deserves further investigation. The present study indicates a promising anticancer effect of AA that is dependent on cell properties such as the basal redox state of the cancer and normal cells. The present study also reveals cell-dependent ROS generation in AA treatment and identifies the RelB-SIRT3-MnSOD axis as a critical contributor to AA-induced radiosensitization of cancer cells and radioprotection of normal cells (Fig. 7D). Thus, while additional mechanistic studies are needed to fully understand the biological function of AA, we anticipate that other redox-based anticancer therapeutics with protective properties against cytotoxic therapy will be discovered and that they will have a significant impact on the care of cancer patients.

Supplementary Material

Refer to Web version on PubMed Central for supplementary material.

Acknowledgments

Funding source: This work was supported mainly by NIH grants CA 049797 and CA 143428 to DK St Clair and WH St Clair. Additional support was provided by grants from the National Natural Science Foundation of China (Grant No. 81272469) and the Natural Science Foundation of Jiangsu Province (Grant No. BL2012016) to J Chen. The research used service facilities funded by a Cancer Center support grant (P30 CA177558).

The authors thank Dr. Mike Mitov and Mr. Michael Alstott of the Redox Metabolism Service Facility at the University of Kentucky, who provided technical support for the Seahorse experiments.

References

1. Siegel RL, Miller KD, Jemal A. Cancer statistics, 2015. CA Cancer J Clin. 2015; 65:5–29. [PubMed: 25559415]
2. Al-Mamgani A, Lebesque JV, Heemsbergen WD, Tans L, Kirkels WJ, Levendag PC, et al. Controversies in the treatment of high-risk prostate cancer: what is the optimal combination of hormonal therapy and radiotherapy: a review of literature. Prostate. 2010; 70:701–9. [PubMed: 20017166]
3. Nichol A, Chung P, Lockwood G, Rosewall T, Divanbiegi L, Sweet J, et al. A phase II study of localized prostate cancer treated to 75. 6 Gy with 3D conformal radiotherapy. Radiother Oncol. 2005; 76:11–17. [PubMed: 15990187]
4. Beckendorf V, Guerif S, Le Prisé E, Cosset JM, Bougnoux A, Chauvet B, et al. 70 Gy versus 80 Gy in localized prostate cancer: 5-year results of GETUG 06 randomized trial. Int J Radiat Oncol Biol Phys. 2011; 80:1056–63. [PubMed: 21147514]
5. Azzam EI, Jay-Gerin JP, Pain D. Ionizing radiation-induced metabolic oxidative stress and prolonged cell injury. Cancer Lett. 2012; 327:48–60. [PubMed: 22182453]
6. Skvortsova I, Debbage P, Kumar V, Skvortsov S. Radiation resistance: Cancer stem cells (CSCs) and their enigmatic pro-survival signaling. Semin Cancer Biol. 2015; 35:39–44. [PubMed: 26392376]
7. Droge W. Free radicals in the physiological control of cell function, Physiol. Rev. 2002; 82:47–95.
8. Tang FR, Loke WK. Molecular mechanisms of low dose ionizing radiation-induced hormesis, adaptive responses, radioresistance, bystander effects, and genomic instability. Int J Radiat Biol. 2015; 91:13–27. [PubMed: 24975555]
9. Creagan ET, Moertel CG, O'Fallon JR, Schutt AJ, O'Connell MJ, Rubin J, et al. Failure of high-dose vitamin C (ascorbic acid) therapy to benefit patients with advanced cancer. A controlled trial. N Engl J Med. 1979; 301:687–90. [PubMed: 384241]
10. Chen Q, Polireddy K, Chen P, Dong R. The unpaved journey of vitamin C in cancer treatment. Can J Physiol Pharmacol. 2015; 93:1055–63. [PubMed: 26469874]
11. Padayatty SJ, Sun H, Wang Y, Riordan HD, Hewitt SM, Katz A, Wesley RA, et al. Vitamin C pharmacokinetics: Implications for oral and intravenous use. Ann Intern Med. 2004; 140:533–37. [PubMed: 15068981]
12. Monti DA, Mitchell E, Bazzan AJ, Littman S, Zabrecky G, Yeo CJ, et al. Phase I evaluation of intravenous ascorbic acid in combination with gemcitabine and erlotinib in patients with metastatic pancreatic cancer. PLoS One. 2012; 7:e29794. [PubMed: 22272248]
13. Welsh JL, Wagner BA, Van't Erve TJ, Zehr PS, Berg DJ, Halfdanarson TR, et al. Pharmacological ascorbate with gemcitabine for the control of metastatic and node-positive pancreatic cancer (PACMAN): results from a phase I clinical trial. Cancer Chemother Pharmacol. 2013 Mar.71:765–75. [PubMed: 23381814]
14. Chen Q, Espey MG, Sun AY, Lee JH, Krishna MC, Shacter E, et al. Ascorbate in pharmacologic concentrations selectively generates ascorbate radical and hydrogen peroxide in extracellular fluid in vivo. Proc Natl Acad Sci USA. 2007; 104:8749–54. [PubMed: 17502596]

15. Du J, Martin SM, Levine M, Wagner BA, Buettner GR, Wang SH, et al. Mechanisms of ascorbate-induced cytotoxicity in pancreatic cancer. Clin Cancer Res. 2010; 16:509–20. [PubMed: 20068072]
16. Ahmed KM, Zhang H, Park CC. NF-κB regulates radioresistance mediated by β1-integrin in three-dimensional culture of breast cancer cells. Cancer Res. 2013; 73:3737–48. [PubMed: 23576567]
17. Lessard L, Bégin LR, Gleave ME, Mes-Masson AM, Saad F. Nuclear localisation of nuclear factor-kB transcription factors in prostate cancer: an immunohistochemical study. Br J Cancer. 2005; 93:1019–23. [PubMed: 16205698]
18. Xu Y, Fang F, Sun Y, St Clair DK, St Clair WH. RelB-dependent differential radiosensitization effect of STI571 on prostate cancer cells. Mol Cancer Ther. 2010; 9:803–12. [PubMed: 20371728]
19. Stephenson CM, Levin RD, Spector T, Lis CG. Phase I clinical trial to evaluate the safety, tolerability, and pharmacokinetics of high-dose intravenous ascorbic acid in patients with advanced cancer. Cancer Chemother Pharmacol. 2013; 72:139–46. [PubMed: 23670640]
20. Chou TC. Drug combination studies and their synergy quantification using the Chou-Talalay method. Cancer Res. 2010; 70:440–46. [PubMed: 20068163]
21. Xu Y, Josson S, Fang F, St Clair DK, Wan XS, Sun Y, et al. RelB enhances prostate cancer growth: implications for the role of the NF-kB alternative pathway in tumorigenicity. Cancer Res. 2009; 69:3267–71. [PubMed: 19351823]
22. Hoffer LJ, Levine M, Assouline S, Melnychuk D, Padayatty SJ, Rosadiuk K, et al. Phase I clinical trial of i.v. ascorbic acid in advanced malignancy. Ann Oncol. 2008; 19:1969–74. [PubMed: 18544557]
23. Weydert CJ, Waugh TA, Ritchie JM, Iyer KS, Smith JL, Li L, Spitz DR, Oberley LW. Overexpression of manganese or copper zinc superoxide dismutase inhibits breast cancer growth. Free Radic Biol Med. 2006; 41:226–237. [PubMed: 16814103]
24. Weydert C, Roling B, Liu J, Hinkhouse MM, Ritchie JM, Oberley LW, Cullen JJ. Suppression of the malignant phenotype in human pancreatic cancer cells by the overexpression of manganese superoxide dismutase. Mol Cancer Ther. 2003; 2:361–369. [PubMed: 12700280]
25. Liu R, Fan M, Candas D, Qin L, Zhang X, Eldridge A, et al. CDK1-Mediated SIRT3 Activation Enhances Mitochondrial Function and Tumor Radioresistance. Mol Cancer Ther. 2015; 14:2090–102. [PubMed: 26141949]
26. Xu Y, Fang F, Miriyala S, Crooks PA, Oberley TD, Chaiswing L, et al. KEAP1 is a redox sensitive target that arbitrates the opposing radiosensitive effects of parthenolide in normal and cancer cells. Cancer Res. 2013; 73(14):4406–17. [PubMed: 23674500]
27. Sun Y, St Clair DK, Fang F, Warren GW, Rangnekar VM, Crooks PA, et al. The radiosensitization effect of parthenolide in prostate cancer cells is mediated by nuclear factor-kappaB inhibition and enhanced by the presence of PTEN. Mol Cancer Ther. 2007; 6:2477–86. [PubMed: 17876045]
28. Yun J, Mullarky E, Lu C, Bosch KN, Kavalier A, Rivera K, et al. Vitamin C selectively kills KRAS and BRAF mutant colorectal cancer cells by targeting GAPDH. Science. 2015; 350:1391–96. [PubMed: 26541605]
29. Morgan MJ, Liu ZG. Crosstalk of reactive oxygen species and NF-κB signaling. Cell Res. 2011; 21:103–15. [PubMed: 21187859]
30. Holley AK, Xu Y, St Clair DK, St Clair WH. RelB regulates manganese superoxide dismutase gene and resistance to ionizing radiation of prostate cancer cells. Ann N Y Acad Sci. 2010; 1201:129–36. [PubMed: 20649549]
31. Liu TF, Vachharajani V, Millet P, Bharadwaj MS, Molina AJ, McCall CE. Sequential actions of SIRT1-RELB-SIRT3 coordinate nuclear-mitochondrial communication during immunometabolic adaptation to acute inflammation and sepsis. J Biol Chem. 2015; 290:396–408. [PubMed: 25404738]
32. Davis-Yadley AH, Malafa MP. Vitamins in Pancreatic Cancer: A Review of Underlying Mechanisms and Future Applications. Adv Nutr. 2015; 6:774–802. [PubMed: 26567201]
33. Du J, Cieslak JA 3rd, Welsh JL, Sibenaller ZA, Allen BG, Wagner BA, Kalen AL, Doskey CM, Strother RK, Button AM, Mott SL, Smith B, Tsai S, Mezhir J, Goswami PC, Spitz DR, Buettner GR, Cullen JJ. Pharmacological Ascorbate Radiosensitizes Pancreatic Cancer. Cancer Res. 2015 Aug 15; 75(16):3314–26. [PubMed: 26081808]

34. O'Connor MK, Malone JF, Moriarty M, Mulgrew S. A radioprotective effect of vitamin C observed in Chinese hamster ovary cells. Br J Radiol. 1977; 50:587–91. [PubMed: 890235]
35. Hosokawa Y, Monzen S, Yoshino H, Terashima S, Nakano M, Toshima K, et al. Effects of X-ray irradiation in combination with ascorbic acid on tumor control. Mol Med Rep. 2015; 12:5449–54. [PubMed: 26238154]
36. Halperin EC, Gaspar L, George S, Darr D, Pinnell S. A double-blind, randomized, prospective trial to evaluate topical vitamin C solution for the prevention of radiation dermatitis. CNS Cancer Consortium. Int J Radiat Oncol Biol Phys. 26:413–16. 199.
37. Han SS, Kim K, Hahm ER, Lee SJ, Surh YJ, Park HK, et al. L-ascorbic acid represses constitutive activation of NF-kappaB and COX-2 expression in human acute myeloid leukemia, HL-60. J Cell Biochem. 2004; 93:257–70. [PubMed: 15368354]
38. Cárcamo JM1, Pedraza A, Bórquez-Ojeda O, Zhang B, Sanchez R, Golde DW. Vitamin C is a kinase inhibitor: dehydroascorbic acid inhibits IkappaBalpha kinase beta. Mol Cell Biol. 2004; 24:6645–52. [PubMed: 15254232]
39. Bren GD, Solan NJ, Miyoshi H, Pennington KN, Pobst LJ, Paya CV. Transcription of the RelB gene is regulated by NF-kappaB. Oncogene. 2001; 20:7722–33. [PubMed: 11753650]
40. Uetaki M, Tabata S, Nakasuka F, Soga T, Tomita M. Metabolomic alterations in human cancer cells by vitamin C-induced oxidative stress. Sci Rep. 2015; 5:13896. [PubMed: 26350063]
41. Weinberg F, Chandel NS. Mitochondrial metabolism and cancer. Ann NY Acad Sci. 2009; 1177:66–73. [PubMed: 19845608]
42. Viale A, Pettazzoni P, Lyssiotis CA, Ying H, Sánchez N, Marchesini M, Carugo A, Green T, Seth S, Giuliani V, Kost-Alimova M, Muller F, Colla S, Nezi L, Genovese G, Deem AK, Kapoor A, Yao W, Brunetto E, Kang Y, Yuan M, Asara JM, Wang YA, Heffernan TP, Kimmelman AC, Wang H, Fleming JB, Cantley LC, DePinho RA, Draetta GF. Oncogene ablation-resistant pancreatic cancer cells depend on mitochondrial function. Nature. 2014 Oct 30; 514(7524):628–32. [PubMed: 25119024]
43. Schumacker PT. A tumor suppressor SIRTainty. Cancer Cell. 2010; 17:5–6. [PubMed: 20129243]
44. Wu YT, Wu SB, Wei YH. Roles of sirtuins in the regulation of antioxidant defense and bioenergetic function of mitochondria under oxidative stress. Free Radic Res. 2014; 48(9):1070–84. [PubMed: 24797412]
45. Parihar P, Solanki I, Mansuri ML, Parihar MS. Mitochondrial sirtuins: emerging roles in metabolic regulations, energy homeostasis and diseases. Exp Gerontol. 2015 Jan.61:130–41. [PubMed: 25482473]
46. Someya S, Yu W, Hallows WC, Xu J, Vann JM, Leeuwenburgh C, et al. Sirt3 mediates reduction of oxidative damage and prevention of age-related hearing loss under caloric restriction. Cell. 2010; 143:802–12. [PubMed: 21094524]
47. Alhazzazi TY, Kamarajan P, Joo N, Huang JY, Verdin E, D'Silva NJ, et al. Sirtuin-3 (SIRT3), a novel potential therapeutic target for oral cancer. Cancer. 2011; 117:1670–78. [PubMed: 21472714]
48. Tao R, Coleman MC, Pennington JD, Ozden O, Park SH, Jiang H, Kim HS, Flynn CR, Hill S, Hayes McDonald W, Olivier AK, Spitz DR, Gius D. Sirt3-mediated deacetylation of evolutionarily conserved lysine 122 regulates MnSOD activity in response to stress. Mol Cell. 2010 Dec 22; 40(6):893–904. [PubMed: 21172655]
49. Chen Q, Espey MG, Krishna MC, Mitchell JB, Corpe CP, Buettner GR, et al. Pharmacologic ascorbic acid concentrations selectively kill cancer cells: action as a pro-drug to deliver hydrogen peroxide to tissues. Proc Natl Acad Sci USA. 2005; 102:13604–609. [PubMed: 16157892]
50. Welsh JL, Wagner BA, van't Erve TJ, Zehr PS, Berg DJ, Halfdanarson TR, Yee NS, Bodeker KL, Du J, Roberts LJ 2nd, Drisko J, Levine M, Buettner GR, Cullen JJ. Pharmacological ascorbate with gemcitabine for the control of metastatic and node-positive pancreatic cancer (PACMAN): results from a phase I clinical trial. Cancer Chemother Pharmacol. 2013 Mar; 71(3):765–75. [PubMed: 23381814]

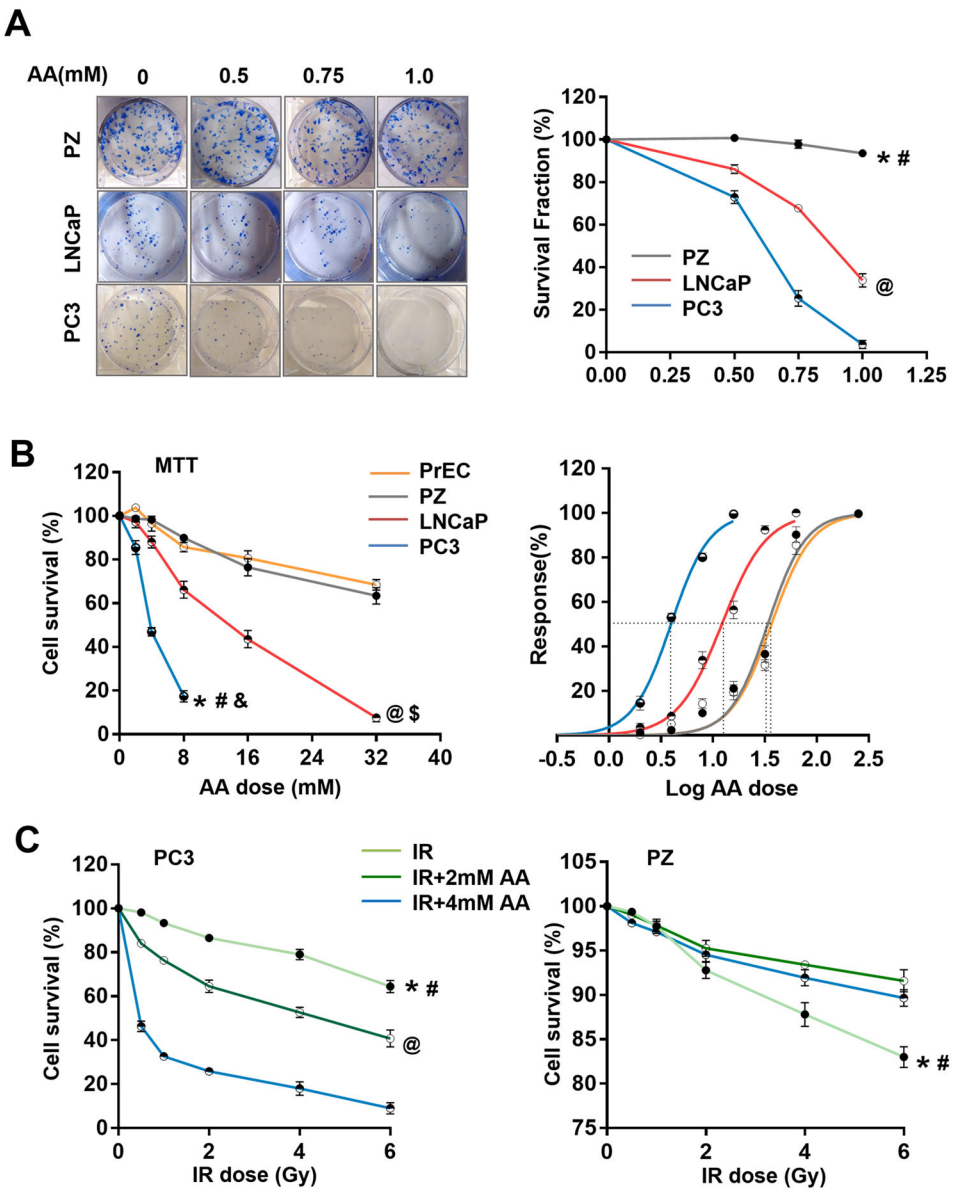

Figure 1.

The effect of AA on proliferation and radiosensitivity of prostate cancer and normal cells. A, Two prostate cancer cell lines (PC3 and LNCaP) and one prostate epithelial cell line (PZ) were treated with different concentrations of AA. Cell survival fraction was determined by colony survival analysis. *, # P<0.001 comparing PZ cells to PC3 (*) and LNCaP (#) cells, respectively. @ P<0.001 comparing LNCaP and PC3 cells. B, Two prostate cancer cell lines (PC3 and LNCaP) and two prostate epithelial cell lines (PZ and PrEC) were treated with different concentrations of AA. Cell survival fraction was determined by MTT assay. IC_{50} for each cell line was calculated based on the dose-response curve. *, #, & P<0.001 comparing PC3 cells to PZ (*), LNCaP (#) and PrEC (&) cells, respectively. @, $ P<0.001 comparing LNCaP cells to PZ (@) and PrEC ($) cells, respectively. C, Prostate cancer PC3 cells and prostate epithelial PZ cells were treated with IR and AA at indicated doses. Cell

survival fraction was determined by MTT assay. *, # P<0.001 comparing IR group to IR +2mM (#) and IR+4mM (*) groups, respectively. @ P<0.001 comparing IR+2mM and IR +4mM groups. All the analyses were performed using linear regression models and Likelihood ratio tests with Bonferroni correction.

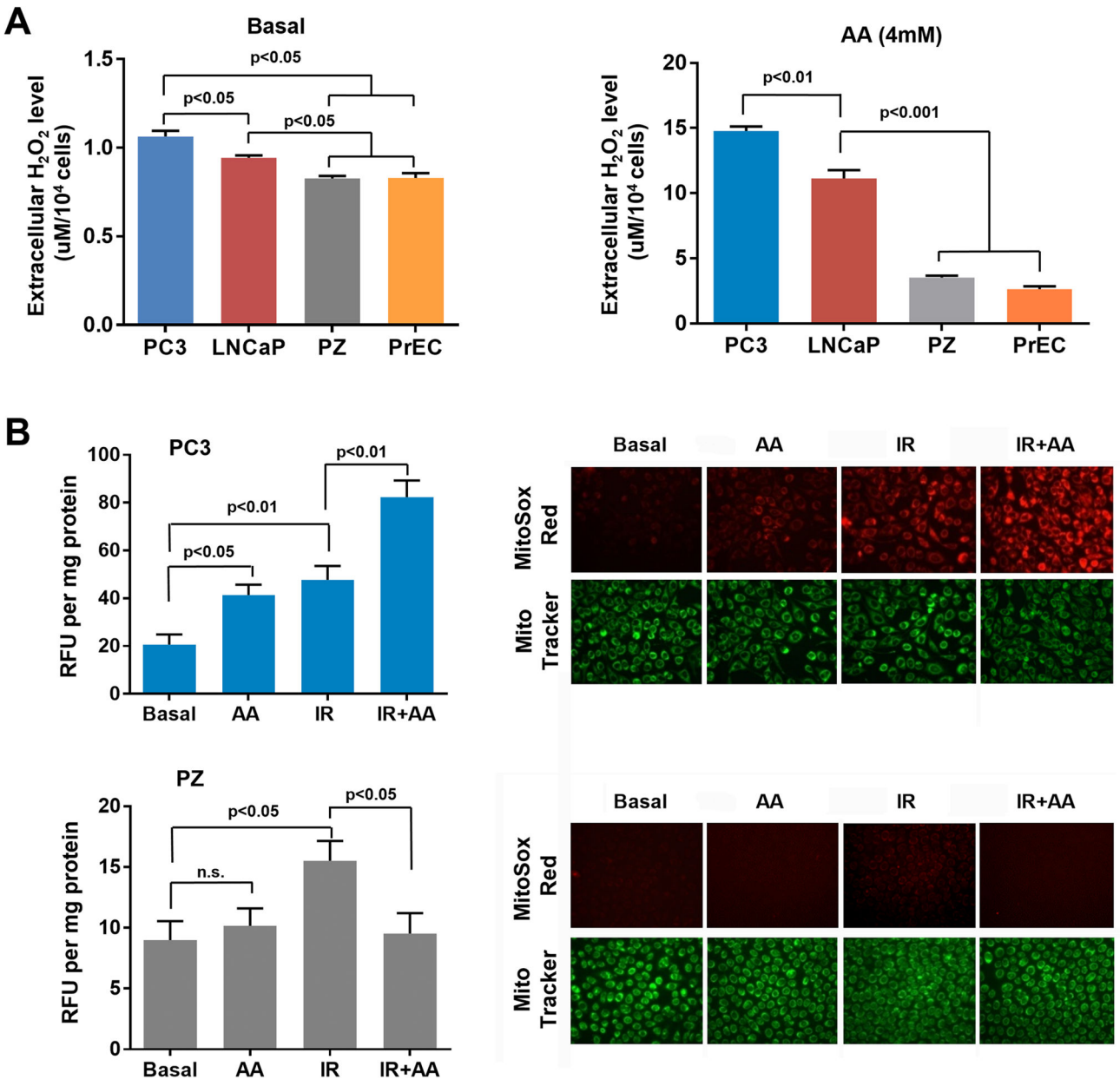

Figure 2.

The effect of AA on redox homeostasis in prostate cancer and normal cells. A, Prostate cancer and normal epithelial cells were treated with AA and then incubated with Amplex Red. The extracellular H_2O_2 concentration was calculated by a standard curve and normalized to the cell number. B, Concentrations of mitochondrial superoxide in PC3 and PZ cells were measured by MitoSox Red after treatment with AA and IR as indicated. Cellular fluorescence intensity was detected by fluorescence microscopy and a fluorescence microplate reader. Mitochondria were visualized by staining with Mitotracker Green. Microplate readings were normalized by protein levels. n.s, no significance detected. All the analyses were performed using one-way ANOVA with post-hoc Tukey HSD test.

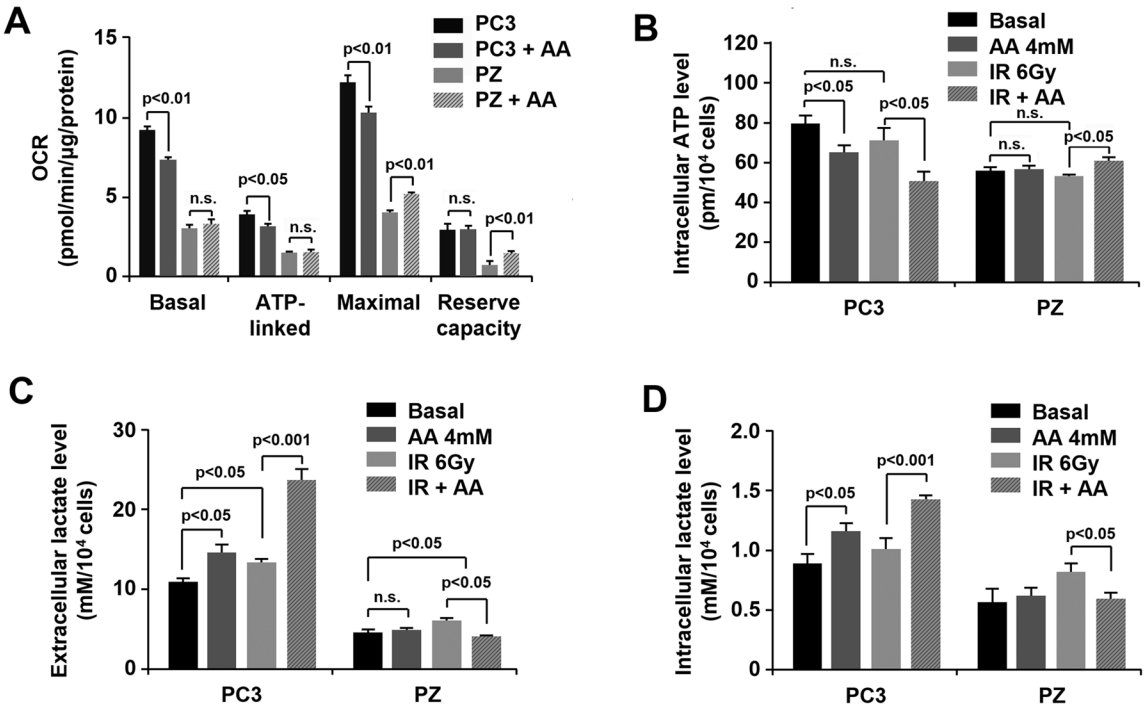

Figure 3.

The effect of AA on metabolic homeostasis in prostate cancer and normal cells. A, After AA treatment, OCR in PC3 and PZ cells was measured by a Seahorse Bioscience XF96 OxygenFlux Analyzer. B, Intracellular ATP levels were measured after treatment with AA and IR at the indicated doses. C and D, Extracellular and intracellular lactate levels. Two-tailed Student's t test was performed for comparisons of treated groups to control groups in OCR test. One-way ANOVA with post-hoc Tukey HSD test was performed for comparisons of multiple groups in cells. n.s. represents non-statistical significance.

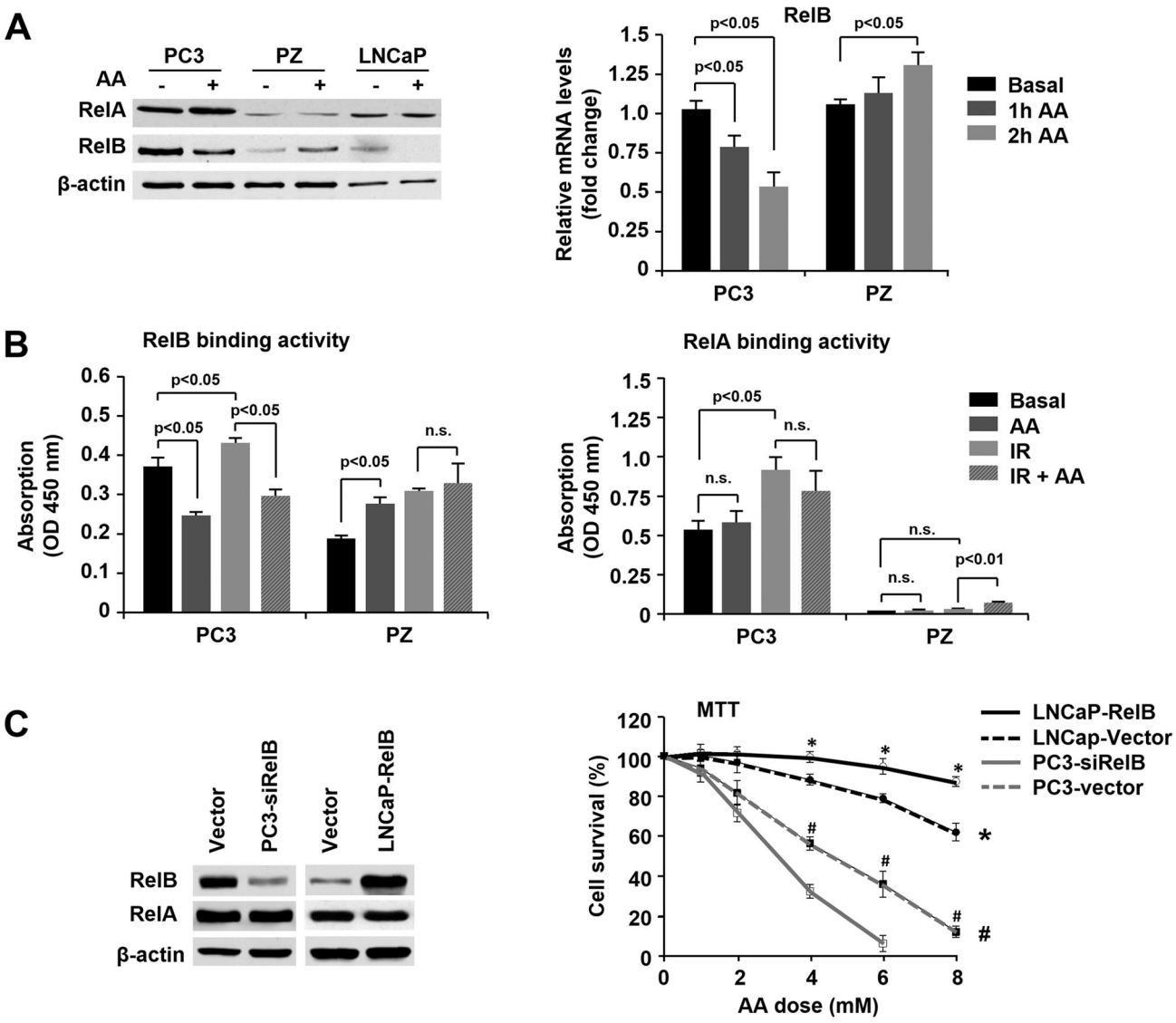

Figure 4.

Differential regulation of RelB by AA in prostate cancer and normal cells. A, After AA treatment, the expression levels of RelA and RelB were quantified by western blots and RT-PCR. B, Nuclear extracts from the treated and untreated cells were subjected to the NF-κB binding assay kit. Binding activities of RelA and RelB were determined by ELISA analysis. C, RelB was overexpressed in LNCaP cells and silenced in PC3 cells by cell transfection, and the cells were treated with different concentrations of AA. Cell survival fraction was determined by MTT assay. * P<0.001 comparing LNCaP-RelB and LNCaP-Vector cells; # P<0.001 comparing PC3-siRelB and PC3-Vector cells based on Linear regression models and Likelihood ratio tests with Bonferroni correction. Other data were analyzed using one-way ANOVA with post-hoc Tukey HSD test.

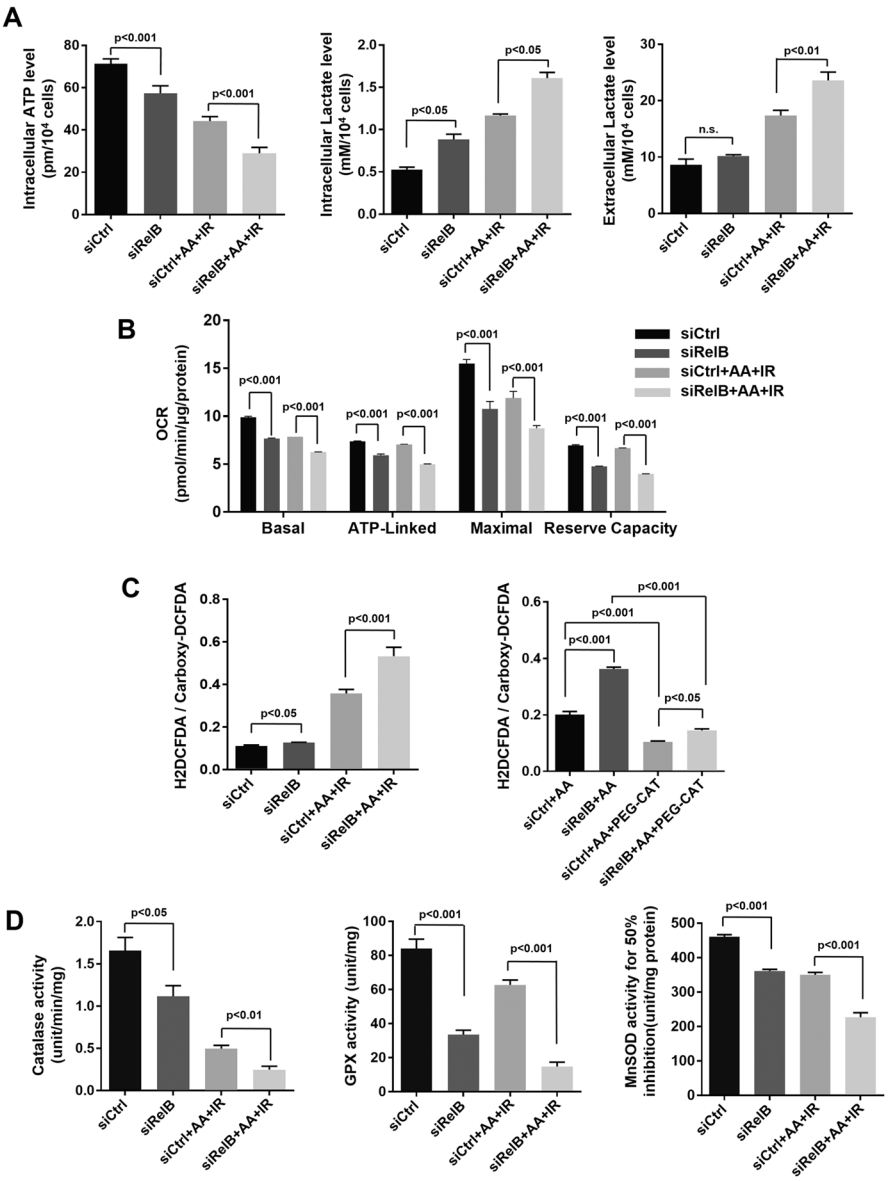

Figure 5.

The regulation of RelB on redox and metabolic homeostasis. A, Intracellular ATP levels, extracellular and intracellular lactate levels were measured after treatment with AA and IR at the indicated doses in PC3 and in RelB-silenced PC3 cells. B, After AA and IR treatment, OCR in PC3 and in RelB-silenced PC3 cells was measured by a Seahorse Bioscience XF96 OxygenFlux Analyzer. C, The level of cellular ROS was estimated by the ratio of H2DCFDA to Carboxy-DCFDA. PEG-Catalase was used as a control to remove ROS generated by AA. D, Catalase activity, Gpx activity and MnSOD activity were measured after treatment with AA and IR in PC3 and in RelB-silenced PC3 cells. Two-tailed Student's t test was performed for comparisons of RelB- silenced group to control group.

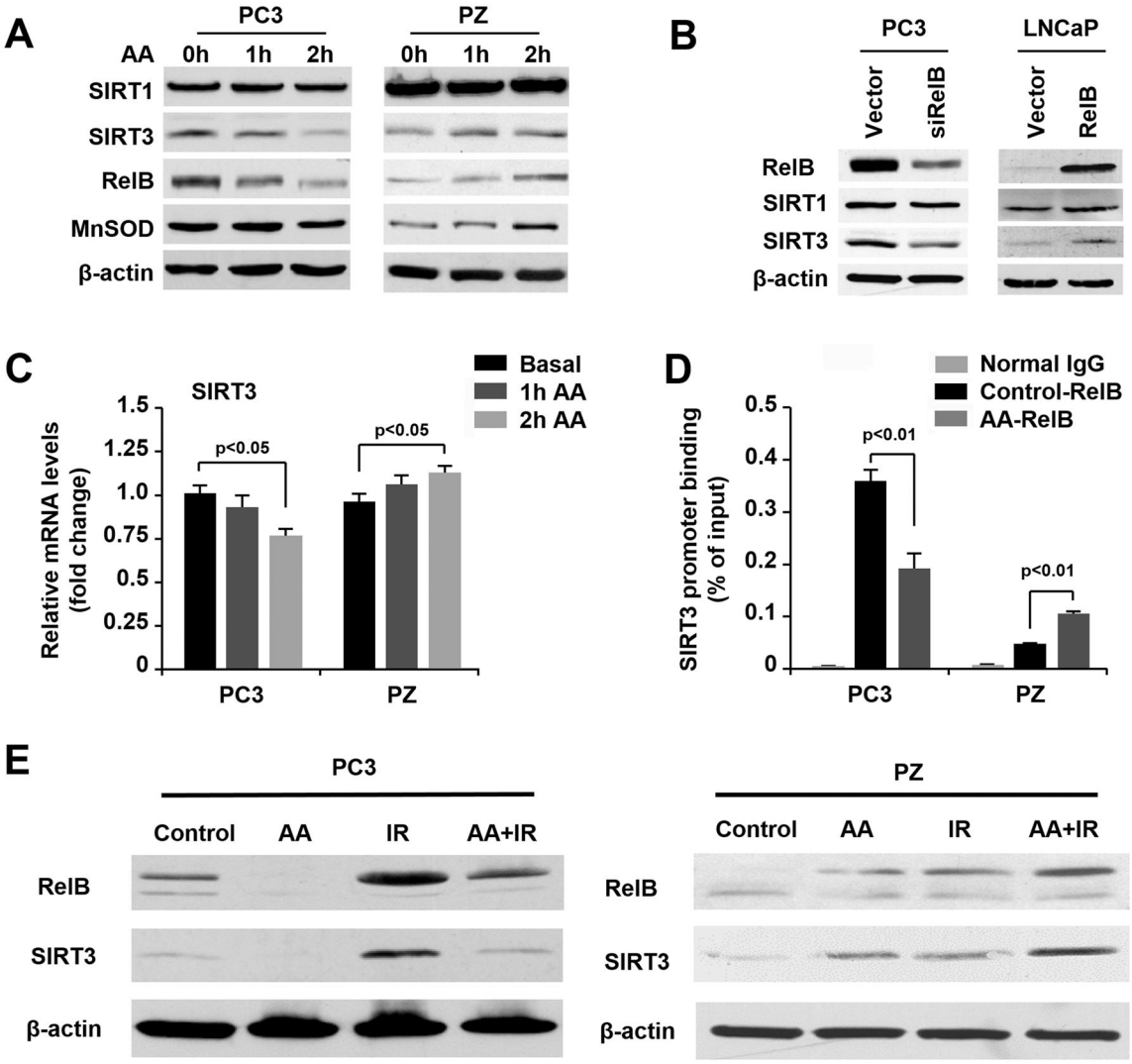

Figure 6.

Modulation of SIRT3 due to AA-mediated RelB regulation. A, After AA treatment, the expression of SIRT1, SIRT3, RelB, and MnSOD in PC3 and PZ cells was measured by western blots. B, Protein levels of SIRT1 and SIRT3 after manipulation of RelB expression in LNCaP and PC3 cells were determined by western blots. C, After AA treatment, mRNA levels of SIRT3 in PC3 cells and PZ cells were determined by RT-PCR. D, Protein–DNA complexes were extracted from the AA-treated or untreated PC3 and PZ cells and then immunoprecipitated using a RelB antibody. The SIRT3 promoter fragment containing a NF-κB element was amplified by q-PCR with specific primers, which were normalized by their input controls containing relevant unprecipitated chromatin. E, After AA and radiation treatment, the expression of RelB-SIRT3 in PC3 and PZ cells was measured by western blots. One-way ANOVA with post-hoc Tukey HSD test was performed for comparison of multiple groups in cells.

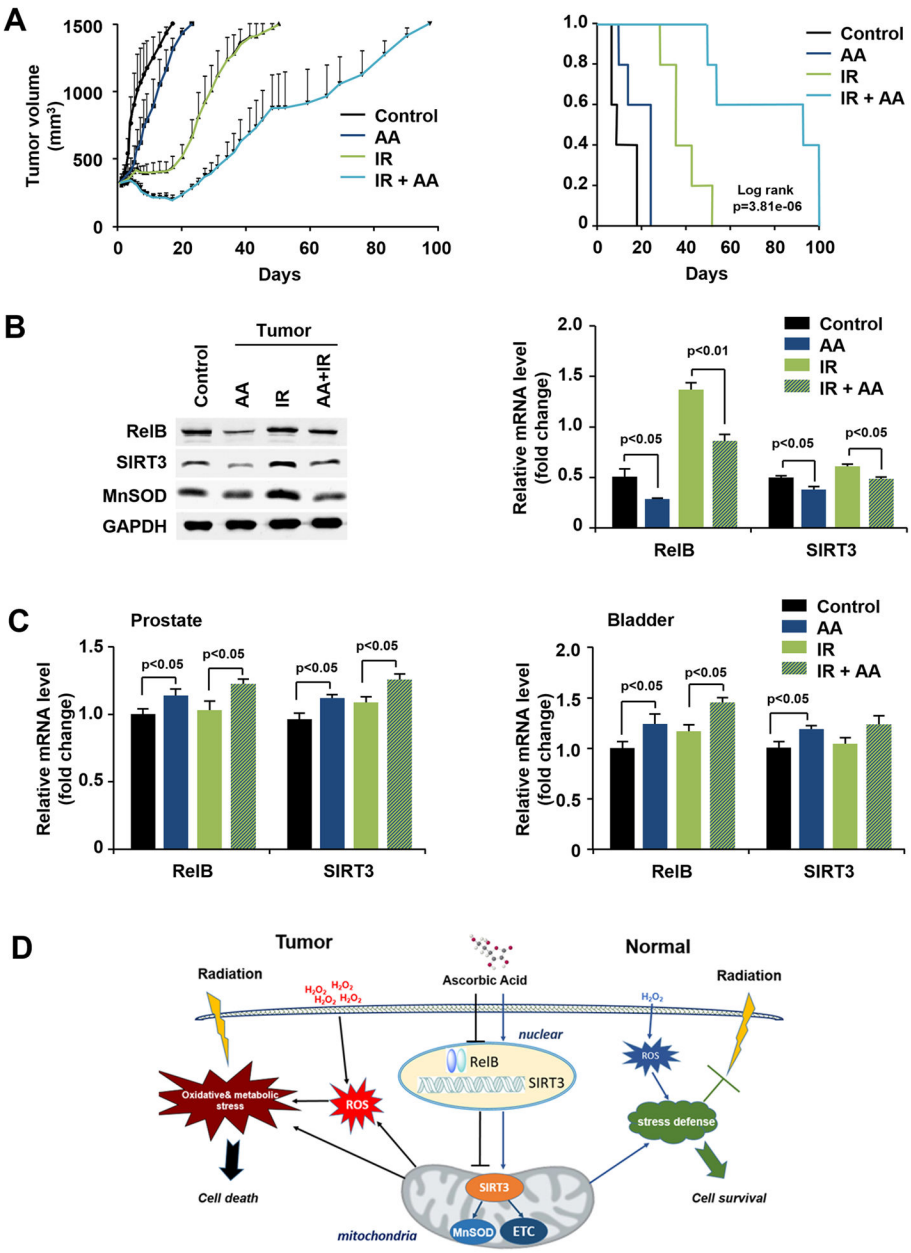

Figure 7.

AA-mediated radiosensitization of prostate cancer cells *in vivo*. A, Prostate cancer PC3 cells were injected into the flanks of nude male mice and the formed tumors were treated with AA and IR as indicated. Tumor volume was measured and tumor growth rate was calculated. Kaplan-Meier survival curves and the log-rank test were performed for comparison of the survival curves. B, The levels of RelB, SIRT3, and MnSOD in tumor tissue were measured by western blots and RT-PCR. C, mRNA levels of RelB and SIRT3 in prostate and bladder tissues were quantified by RT-PCR. D, A proposed mechanistic model for the AA-mediated differential response to radiation in prostate cancer and normal cells. AA sensitizes cancer cells to radiation by down-regulating RelB-SIRT3 signal, which in turn aggravates oxidative

and metabolic stresses. In contrast, in normal prostate epithelial cells, H_2O_2 generated from the redox reaction of AA up-regulates RelB, leading to increased SIRT3 levels, which enhances cellular stress defense systems. Kaplan-Meier survival curves and the log-rank test were performed for comparison of the survival curves in animal experiments. Other data were analyzed using one-way ANOVA with post-hoc Tukey HSD test.